PHYSICAL REVIEW B VOLUME 23, NUMBER 8 15 APRIL 1981

Complex band structure and superlattice electronic states

J. N. Schulman* and T. C. McGill
California Institute of Technology, Pasadena, California 91125
(Received 11 February 1980)

The complex band structures of the bulk materials which constitute the alternating layer (001) semiconductor-semiconductor superlattice are investigated. The complex bands near the center of the Brillouin zone in the [001] direction are studied in detail. The decay lengths of superlattice states whose energies lie in the bulk band gaps of one of the semiconductors are determined from the dispersion curves of these bands for imaginary $\vec{k}$. This method is applied using a tight-binding band-structure calculation to two superlattices: the AlAs-GaAs superlattice and the CdTe-HgTe superlattice. The decay lengths of AlAs-GaAs superlattice conduction-band minimum states are found to be substantially shorter than those for the CdTe-HgTe superlattice. These differences in the decay of the states in the two superlattices result in differences in the variation of the conduction-band effective masses with the thickness of the AlAs and CdTe layers. The conduction-band effective masses increase more rapidly with AlAs thickness in the AlAs-GaAs superlattice than with CdTe thickness in the CdTe-HgTe superlattice.

I. INTRODUCTION

Semiconductor superlattices have been the subject of much interest in recent years due to the development of new highly controllable growth techniques, especially molecular beam epitaxy.[1-3] The superlattices consist of alternating layers of two bulk semiconductors having the same crystal structures and similar lattice constants. Two superlattices have been studied in detail both theoretically and experimentally so far. These are the $Al_xGa_{1-x}As$-GaAs and the $In_{1-x}Ga_xAs$-$GaSb_{1-y}As_y$ superlattices.[1-3] In addition, a theoretical calculation of the electronic structure of the CdTe-HgTe superlattice has been carried out.[4]

This paper is concerned with understanding in detail an important feature of some of the electronic states in a superlattice: the decay in space of the electron wave function from one layer into the other. We are, in particular, interested in this effect as it applies to the states at the valence- and conduction-band edges of the superlattice, the states important in determining electronic transport properties in the direction perpendicular to the interface planes.

For superlattices which have alternating slabs consisting of many atomic layers, the effect of the decaying states can be interpreted in terms of the familiar well model for the superlattice. The band gap of one of the bulk constituent semiconductors is envisioned as forming barriers to carriers in wells consisting of allowed energy regions in the other bulk semiconductor. The electronic state decays into the barrier semiconductor. When considering superlattices consisting of a small number of atomic layers, the well model can no longer be used. It is necessary to take into account the microscopic atomic potential and the detailed band structures of the bulk semiconductors.

In this paper we calculate band structures for complex $\vec{k}$ near $\vec{k}=0$ using the empirical tight-binding method. The band structures are then used to investigate the decay lengths of the $\vec{k}=0$ superlattice states of two systems: the AlAs-GaAs and CdTe-HgTe superlattices. The superlattices are constructed parallel to (001) zinc-blende planes. The influence of the bulk band structures of the constituent semiconductors and the differing band line-ups in the two systems on perpendicular superlattice transport is studied and discussed.

The paper is organized as follows. Section II discusses the qualitative physics involved with complex band structures and how they determine decay lengths. It also describes briefly the tight-binding method used to calculate the band structures. Section III describes the complex bulk band structures of CdTe and AlAs. Section IV discusses the electronic states of the two superlattices and relates them to the complex bulk band structures. Section V compares the effective masses of the two superlattices.

II. QUALITATIVE PHYSICS

As mentioned in the preceding section, there exist electronic states of the superlattice with energies which lie in forbidden energy regions of one of the bulk constituent semiconductors. This is illustrated in Fig. 1. It shows a schematic band diagram for a hypothetical superlattice made from two semiconductors labeled 1 and 2. The two materials alternate in the z direction. The bulk valence- and conduction-band edges of each are shown. The hatched area represents the forbidden band gap of the bulk semiconductors (not of the superlattice). The energy E_s is the energy of a

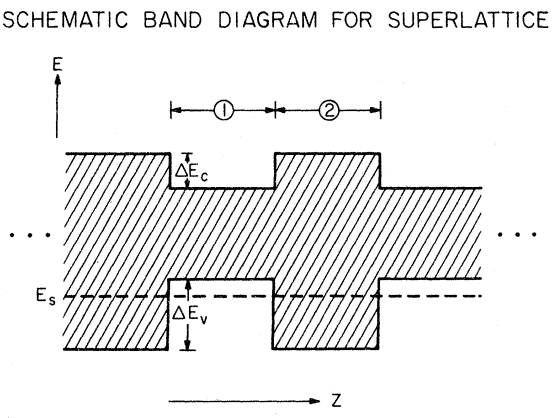

FIG. 1. Schematic band diagram of a hypothetical superlattice. ΔE_v and ΔE_c are the valence- and conduction-band discontinuities between semiconductors 1 and 2. The hatched area represents the bulk band gaps. E_s is the energy of a superlattice state which decays into semiconductor 2.

superlattice state located below the valence-band edge of semiconductor 1 and above the valence-band edge of semiconductor 2. The wave function of this state would be expected to have a characteristic form. In region 1 it is made up of bulk Bloch and evanescent waves of material 1, producing a peaked envelope structure similar to that of a particle in a well. In region 2 the state would exhibit an exponentially decaying behavior with decay lengths characteristic of evanescent states at that energy in material 2. States of this sort have previously been found in several theoretical calculations on superlattices.[5,6]

It is a good approximation to analyze these superlattice states in terms of bulk Bloch and evanescent waves for the following reason. Previous studies have shown that the superlattice potential differs from that of the constituent semiconductors only in short regions near the interfaces, typically within one or two atomic layers.[7] Insofar as the superlattice potential approximates the potential of one or the other of the bulk semiconductors, it is describable by a bulk Hamiltonian in that region. Since Schrödinger's equation is a local equation, its solutions in these regions will be just the bulk solutions. Bulk evanescent states, previously disallowed by the bulk boundary conditions, are now acceptable. The superlattice states are thus well described in terms of the bulk states of the two materials connected at the interfaces.

In this paper we are, in particular, interested in the evanescent states and their decay lengths. The decay lengths to be used depend on two factors: the dispersion of the bulk energy bands as a function of complex $\vec{k}$ and the location in energy of the superlattice state of interest. When both of these are known, the decay length of the evanescent state at the energy of the state in the superlattice is just the reciprocal of the imaginary part of $\vec{k}$, k_i, for that state.

The calculation is simplified by several considerations. Since the superlattices of interest have direct fundamental band gaps, only the band structure near $\vec{k}=0$ must be known. There are other evanescent states away from $\vec{k}=0$ which can connect with the Bloch states at the interface, but they do so only with small amplitudes.[8] We, therefore, do not consider these states. Also, according to Blount,[9] time reversal at $\vec{k}=0$ ensures that all the necessary evanescent states with real energies have purely imaginary values of $\vec{k}$. Thus, the calculation must be done only for $\vec{k}$ near $\vec{k}=0$ in the imaginary [001] direction.

The empirical tight-binding method is used to calculate the band structures in this paper. It has been described in detail in Ref. 5 for the AlAs-GaAs superlattice and in Ref. 4 for the CdTe-HgTe superlattice. The parameters used in the present paper for AlAs-GaAs were obtained from Ref. 8 and those for CdTe-HgTe from Ref. 4. The energies and wave functions of the superlattice states are obtained by diagonalizing the superlattice tight-binding Hamiltonian matrix. The complex bulk band structures are also calculated with the tight-binding method, with the modification that $\vec{k}$ can take on complex as well as real values.

III. COMPLEX BAND STRUCTURE

This section includes the results of our complex band-structure calculations. The theory of complex band structures in three dimensions has been discussed in general terms by Heine.[10] There have been few detailed calculations of this sort done on specific materials because of the difficulty of investigating the complex band structures experimentally. However, since evanescent states are important in determining the tunneling properties of materials, transport measurement involving tunneling through barriers would be useful in investigating complex band structures. This, in fact, was done by Kurtin, McGill, and Mead[11] to determine part of the complex dispersion curves of GaSe by studying tunneling in a metal-insulator-metal structure. Applying complex band-structure considerations to the superlattice yields another, but less direct, system in which to study them. A theoretical study by Osbourn and Smith[8] of transmission and reflection coefficients at $Al_xGa_{1-x}As$-GaAs interfaces also makes use of the complex band structure.

In this paper we are concerned with the com-

plex band structures of the bulk materials which form the "barriers" in Fig. 1. This is AlAs for the AlAs-GaAs superlattice and CdTe for the CdTe-HgTe superlattice. AlAs has a larger direct band gap than GaAs, and it has been experimentally determined to overlap that of GaAs in the superlattice.[12] We use values of ΔE_v and ΔE_c (Fig. 1) equal to 0.19 and 1.10 eV, respectively. Similarly, CdTe has the larger band gap of the CdTe, HgTe pair. HgTe has a band gap of 0 eV due to the degeneracy of the conduction-band minimum and valence-band maximum at $\vec{k}=0$.[13] We use a valence-band discontinuity, ΔE_v, equal to zero for the CdTe-HgTe superlattice for reasons given in a previous paper.[4] Since this superlattice has not yet been fabricated, this value of the discontinuity should be regarded as tentative.

A segment of the band structure of AlAs is shown in Fig. 2. Energy is plotted as a function of k_i, the imaginary part of the wave vector in the [001] direction. The unit of k_i is $2\pi/a$, where a is the AlAs lattice constant (5.66 Å). The real part of $\vec{k}$ is zero in this direction for the energies to be real, as mentioned previously. The arbitrary energy zero is set such that the valence-band maximum of GaAs is at zero. The AlAs valence-band maximum, labeled by its symmetry classification Γ_{15v}, is located $\Delta E_v = 0.19$ eV below this, as shown. The conduction-band minimum is labeled Γ_{1c}.

As explained by Heine,[10] the imaginary dispersion curves connect bands across band gaps at maxima and minima. This can be seen in Fig. 2. The two bands (one doubly degenerate) coming off from the triply degenerate Γ_{15v} level connect to the two conduction-band levels. The value of k_i first increases as the energy increases away from the valence-band maximum. After k_i reaches its maximum value, it then decreases back to zero as the energy approaches the conduction band. The maximum value of k_i for each curve represents the location of a branch point in complex $\vec{k}$ space.[10] The two energies for a given value of k_i on a given curve are the energies on either side of the branch line of that point. The highest energy band in Fig. 2 has no higher band to connect to in our tight-binding approximation. It continues to increase in energy monotonically with k_i.

The complex band structure of CdTe is somewhat more complicated. Crystal symmetry and group theory are enough to determine which bands connect together in the AlAs case. The singly and doubly degenerate valence bands connect with the singly and doubly degenerate conduction bands. The relatively large spin-orbit splitting in CdTe necessitates the inclusion of the spin-orbit interaction in our tight-binding calculation.[4] There is only one single-particle representation of the double symmetry group in the [001] direction and hence, all the states have the same symmetry. We find the bands to be connected as shown in Fig. 3. Again, the curves are labeled at $\vec{k}=0$ by their symmetry classifications there. The zero of energy is at the valence-band maximum. The fundamen-

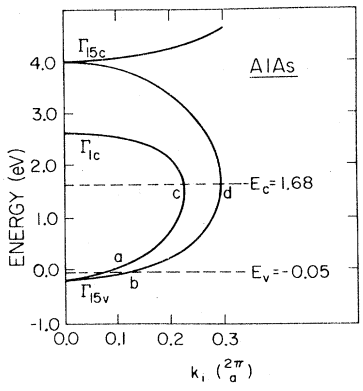

FIG. 2. Complex band structure of AlAs in the [001] direction for purely imaginary $\vec{k}$, k_i. a is the AlAs lattice constant. E_v and E_c indicate the valence-band maximum and conduction-band minimum energies of a superlattice consisting of twenty layers of AlAs alternating with ten layers of GaAs. The points a, b, c, and d label the intersection of these energies with the complex band structure.

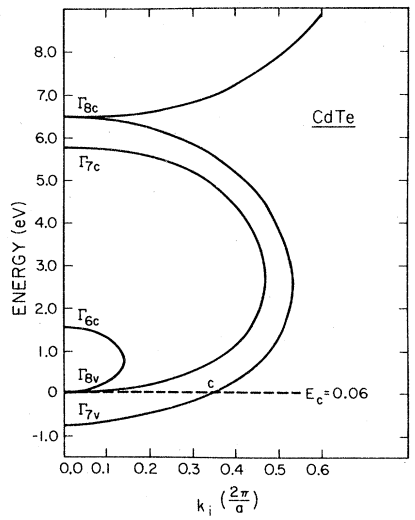

FIG. 3. Complex band structure of CdTe in the [001] direction for purely imaginary $\vec{k}$, k_i. a is the CdTe lattice constant. E_c indicates the conduction-band minimum energy of a superlattice consisting of twenty layers of CdTe alternating with ten layers of HgTe. The point c labels the intersection of this energy with one of the bands.

tal band gap lies between the Γ_{8v} and Γ_{6c} energies. The lattice constant of CdTe is equal to 6.48 Å.

Before going on to relate the superlattice states to the complex band-structure results, it is interesting to examine the applicability of two approximation schemes in determining the complex bands. The first is effective mass theory and the second is a simple adjustment made to take into account the analytic structure of the bands.

It is evident in Figs. 2 and 3 that the parabolic effective-mass approximation can have only a limited range of applicability because the bands eventually turn back towards $\vec{k}=0$ as their energies depart significantly from the band extrema energies. The values of k_i at these points (where $dE/dk_i=\infty$) mark the location of the branch points in the complex band structure. The effective-mass approximation becomes less accurate closer to these points.

We calculated effective masses for small $\vec{k}$ using our tight-binding method and compared the energies resulting from the effective-mass expression with the results of the full tight-binding calculation. The differences in energies are on the order of 10% calculated these two ways for values of k_i near 85% of their branch-point values. The valence bands which connect with these conduction bands are less parabolic and the agreement is only on the order of 30% for the same values of k_i.

A better approximation for these bands is to use a formula which takes into explicit account the existence of the branch points in a simple way. For $\vec{k}$ close to the branch point, the energy must have the characteristic square-root dependence on $\vec{k}$ described by Heine.[10] Such a formula is

$$E=E_0\pm\frac{\hbar^2\gamma}{m_\pm^*}(k^2+\gamma^2)^{1/2} \quad . \tag{1}$$

The parameter γ is equal to the value of k_i at the branch point. E_0 is the energy at that point. The plus or minus sign is chosen depending on whether E is greater or lesser than E_0. The form of Eq. (1) is similar to that derived by Kane[14] using $\vec{k}\cdot\vec{p}$ perturbation theory, with or without the inclusion of the spin-orbit splitting.

The value of γ can be determined from experimentally measurable quantities of the real band structure alone. Setting $k=0$ in Eq. (1) results in two energies whose difference is just the $k=0$ band gap E_g between the two connected bands. Inverting Eq. (1) then implies

$$\gamma=\left\{E_g\Big/\left[\hbar^2\left(\frac{1}{m_+}+\frac{1}{m_-}\right)\right]\right\}^{1/2} \quad . \tag{2}$$

Using the tight-binding derived band gaps and effective masses in Eq. (2) produces values of γ which are almost indistinguishable from those derived from visual inspection of Figs. 2 and 3. A quantitative analysis shows that the tight-binding values differ by only a few percent from those derived from Eq. (2).

IV. SUPERLATTICE STATES

In this section the complex band-structure results are used to analyze the evanescent parts of the superlattice wave functions. First, the superlattice tight-binding method[4,5] is used to find the energies and states for the AlAs-GaAs and Cd-Te-HgTe superlattices. The decay lengths of these states are then compared with the decay lengths of the evanescent bulk states at the same energies.

This procedure is first applied to the AlAs-GaAs superlattice. In particular, the superlattice consisting of twenty layers of AlAs alternating with ten layers of GaAs is considered. The thicker AlAs slabs are used in order to more clearly observe the wave-function decay into the AlAs.

We examine the states at two energies: the conduction-band minimum and the valence-band maximum. The energy of the conduction-band state is 1.68 eV and that of the valence-band state is − 0.05 eV. The two energies are indicated in Fig. 2 by the two dashed lines. It can be seen that the dashed lines for each of these energies intersects the complex dispersion curves at two points. The AlAs states at the intersection points are candidates to match up with the states in the GaAs slabs. The details of how the states connect at the interface determine the amplitude of each bulk AlAs evanescent state in the superlattice state. We do not directly investigate the interface to find these amplitudes. However, the superlattice state at the top of the valence band is doubly degenerate and connects with a doubly degenerate state in AlAs denoted by b in Fig. 2. The superlattice state at the bottom of the conduction band is singly degenerate and connects with a singly degenerate state denoted by c in Fig. 2. In Fig. 4 is plotted the superlattice wave function for the valence-band-maximum state in the AlAs slab only. The state is plotted as a function of layer spacing away from the AlAs-GaAs interface on a logarithmic scale. The integers labeling the horizontal axis are centered about the aluminum atom positions. Layer 1 is at the interface and layer 10 is at the center of the AlAs slab. The lines connecting the dots are for visual aid purposes only. The state has two com-

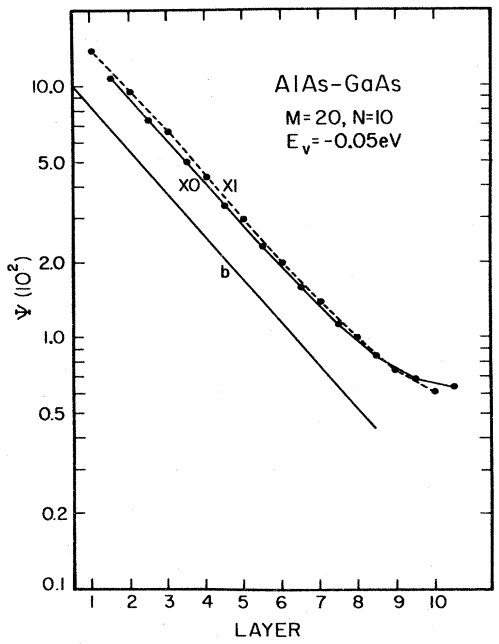

FIG. 4. Wave function of the state at the valence-band maximum of the AlAs-GaAs superlattice in the AlAs slab. The line labeled *b* has the slope given by the decay length of the state at *b* in Fig. 2. *M* and *N* are the number of AlAs and GaAs layers per repeated superlattice slab.

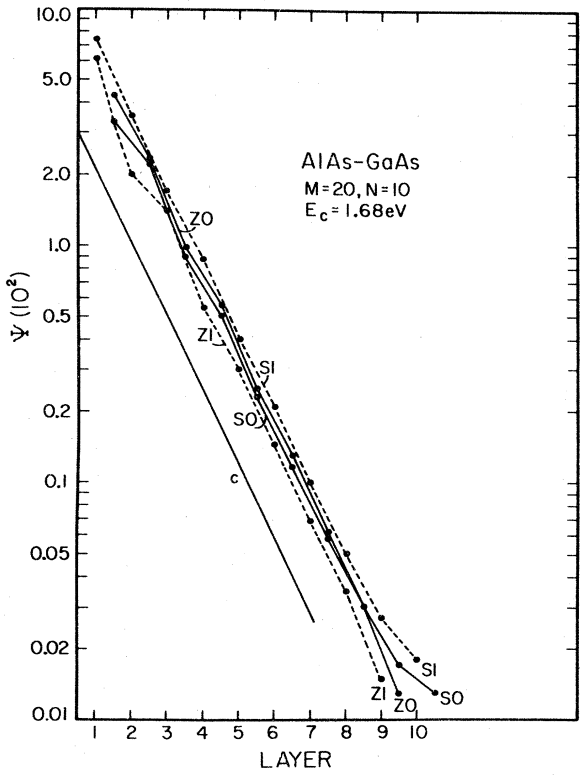

FIG. 5. Wave function of the state at the conduction-band minimum of the AlAs-GaAs superlattice in the AlAs slab. The line labeled *c* has the slope given by the decay length of the state at *c* in Fig. 2. *M* and *N* are the number of AlAs and GaAs layers per repeated superlattice slab.

ponents plotted separately. The solid line labeled *XO* represents the amplitudes of orbitals centered on arsenic atoms with *X*- or *Y*-type symmetry. The dashed line labeled *X*1 represents the same symmetry orbitals on the aluminum atoms. These are the only orbitals allowed by symmetry for this state. Figure 5 is the same type of plot for the conduction-band-minimum state. It is allowed to have orbitals of *S*- and *Z*-type symmetry as indicated.

The decay lengths of the evanescent bulk AlAs states which describe the superlattice states are also shown in Figs. 4 and 5. The straight line shown in Fig. 4 represents the decay length of the state labeled *b* in Fig. 2. Its decay length is 2.55 in units of the layer spacing. The state labeled *a* in Fig. 2 does not have any amplitude in the superlattice state because it is of the improper symmetry type. Similarly, the conduction minimum state in Fig. 5 is well described by just the state labeled *c* in Fig. 2. It has a decay length of 1.40 in the same units. Again, symmetry excludes the bulk state at *d* contributing to the superlattice state. The deviation of the states from an exponential decay near the center of the slab is due to the presence of the decaying state from the next interface.

The situation is more complicated for the CdTe-HgTe superlattice. The states have only one representation due to the necessary inclusion of the spin-orbit interaction. This is illustrated by considering the bottommost conduction state in the superlattice consisting of twenty layers of CdTe and ten of HgTe. The energy of the state is 0.06 eV as indicated by the dashed line in Fig. 3. For greater clarity, the energy range near 0 eV is expanded in Fig. 6. The dashed line is seen to intersect the complex bands at three points labeled *a*, *b*, and *c*.

The question is: How much does each of the three bulk states contribute to the superlattice state at that energy? Since all three states have the same symmetry, all must be considered. The superlattice wave function in the CdTe is shown in Fig. 7. The dashed curves represent amplitudes of orbitals centered on cadmium atoms and the solid curves represent orbitals on tellurium atoms. In addition each curve is labeled by its orbital type (*X* stands for *X* and *Y* orbitals) with 0 and 1 representing cadmium- and tellurium-centered orbitals, respectively. The decay lengths of the bulk evanescent states are represented in the top part of the figure as straight

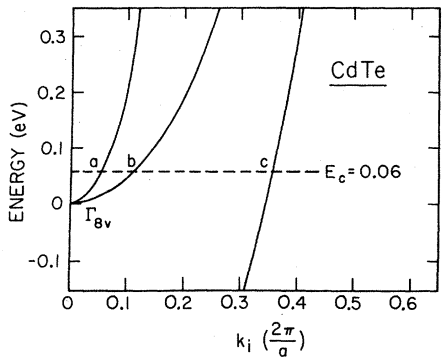

FIG. 6. Expanded version of the CdTe complex bands shown in Fig. 3 near $E=0$. The points a, b, and c label the intersection of the line indicating the superlattice conduction-band minimum energy with the complex band structure.

lines. The states at a in Fig. 6 is on the dispersion curve characterized near $\vec{k}=0$ by the light-hole effective mass. It has a decay length of 5.79 CdTe-layer widths. The state at b originates from the heavy-hole band and it has a decay length of 2.87. Finally, the state at c is from the spin-orbit split-off band, and it has a decay length of 0.90.

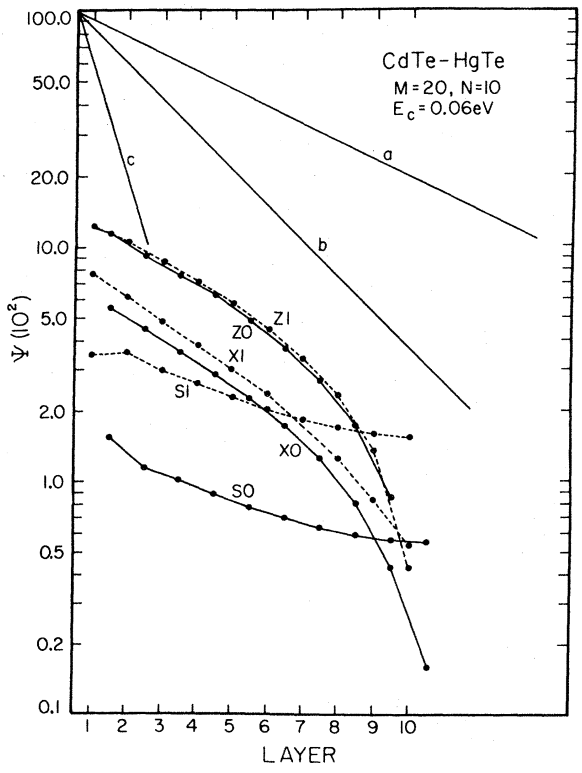

FIG. 7. Wave function of the state at the conduction-band minimum of the CdTe-HgTe superlattice in the CdTe slab. The lines labeled a, b, and c have the slopes given by the decay lengths of the states at a, b, and c in Fig. 6. M and N are the number of CdTe and HgTe layers per repeated superlattice slab.

Different components of the superlattice wave function need to be characterized by different decay lengths. The X, Y, and Z orbital amplitudes are well described by the decay length of the heavy-hole band state at b. The s orbitals have amplitudes with longer decay lengths and are described by the light-hole band state at a. The deviation of the states from exponential decay is again due to the presence of decaying states from the next interface. This effect is more pronounced in the CdTe-HgTe case than in the AlAs-GaAs case because the decay lengths are longer in the CdTe-HgTe case.

V. EFFECTIVE MASSES

The preceding analysis of the decay lengths of the superlattice states leads to important conclusions regarding transport. As discussed in Sec. I, longer decay lengths imply smaller effective masses in the direction perpendicular to the interfaces. We find that there should be relatively small conduction-band effective masses in the CdTe-HgTe superlattice, despite the large conduction-band discontinuity between CdTe and HgTe. This is in contrast to what occurs for the AlAs-GaAs superlattice which also has a large conduction-band discontinuity.

The reason for this involves the close proximity in energy of the CdTe-HgTe superlattice conduction-band minimum to the CdTe bulk valence-band maximum. The conduction band of the superlattice is derived from the HgTe conduction band which is degenerate with the valence-band maximum in the bulk. This property of the conduction-band state in the superlattice combined with the small offset between the valence-band edges of the bulk HgTe and CdTe leads to this close proximity. Because of this proximity the appropriate CdTe evanescent states in the CdTe slabs have small values of k_i, as shown in Fig. 6. The states at a and b have small values of k_i (0.06 and 0.11, respectively) and thus long decay lengths. The AlAs-GaAs superlattice conduction-band energy intersects the relevant dispersion curve in Fig. 2 at c which has a relatively large value of k_i (0.23) and thus a short decay length.

The values of the decay lengths of the conduction-band states for the CdTe-HgTe superlattice are dependent on the precise values of the band discontinuities. Raising the bulk HgTe band structure relative to the CdTe band structure would raise the energy E_c in Fig. 6 and thus change the intersection points with the dispersion curves. This would result in shorter decay

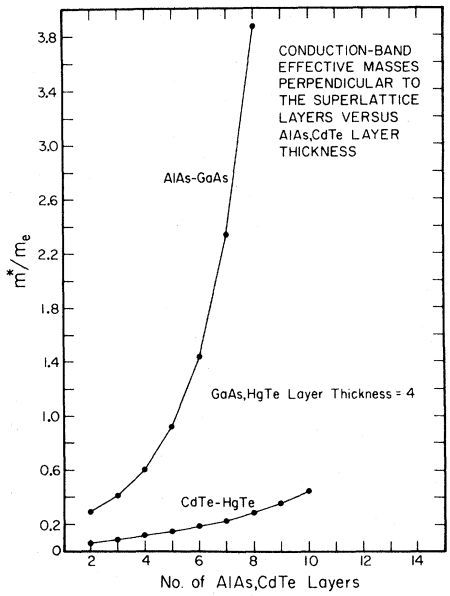

FIG. 8. Conduction-band effective masses perpendicular to the superlattice layers for the AlAs-GaAs and CdTe-HgTe superlattices as a function of the number of AlAs or CdTe atomic layers per slab. There are four layers of GaAs or HgTe per slab.

lengths. The opposite effect would occur from lowering the HgTe band structure. The valence band is similarly effected.

The longer decay lengths in the CdTe-HgTe superlattice indicate that the effective masses should be smaller. This demonstrated in Fig. 8. It shows the conduction-band effective masses for both superlattices as calculated using the superlattice tight-binding method. The masses are plotted as a function of the number of AlAs or CdTe atomic layers per repeated slab. The number of layers of GaAs and HgTe is held constant at four. The AlAs-GaAs effective masses are seen to be substantially larger. Due to the inaccuracy in the values of the bulk tight-binding effective masses, however, this result must be regarded as qualitative only.

The valence-band effective masses show similar trends. The superlattice valence-band-maximum energies are closer to the AlAs or CdTe valence-band edges than is true for the conduction-band energies. Therefore, the valence-state decay lengths are longer and the effective masses grow more slowly with layer thickness. For the same AlAs-GaAs superlattices as those in Fig. 8, the valence-band mass varies from 0.38 for two layers of AlAs to 0.87 for ten layers of AlAs. The topmost valence-band structure of the CdTe-HgTe superlattice consists of a number of bands separated by energies on the order of a meV. These bands interact, making it difficult to assign meaningful effective masses.

VI. SUMMARY

We have calculated the complex band structures of AlAs and CdTe in the [001] direction. A simple formula taking into account the analytic nature of the bands was found which describes the bands well. The band structures were then used to analyze the decay lengths of superlattice states in the "barrier" semiconductor. The effective masses were found to vary rapidly with barrier layer thickness for states having small decay lengths. The effective masses varied more slowly with barrier layer thickness for states with larger decay lengths. For the CdTe-HgTe superlattice, the zero band gap of HgTe combined with the small expected offset in valence-band edges of CdTe and HgTe results in long decay lengths and, consequently, small effective masses for relatively large CdTe layer thickness.

ACKNOWLEDGMENTS

The authors are grateful for many useful discussions with D. L. Smith, G. C. Osbourn, and Y. C. Chang. Equation (1) was brought to our attention by Y. C. Chang. The authors acknowledge the support of ARO under Contract No. DAAG29-77-C-0015.

*Present address: Department of Physics and Astronomy, University of Hawaii, Honolulu, Hawaii.

[1]R. Dingle, A. C. Gossard, and W. Wiegmann, Phys. Rev. Lett. 34, 1327 (1975).
[2]L. L. Chang, L. Esaki, W. E. Howard, R. Ludeke, and G. Schul, J. Vac. Sci. Technol. 10, 655 (1973).
[3]H. Sakaki, L. L. Chang, R. Ludeke, Chin-An Chang, and L. Esaki, Appl. Phys. Lett. 31, 211 (1977).
[4]J. N. Schulman and T. C. McGill, Appl. Phys. Lett. 34, 663 (1979); J. Vac. Sci. Technol. 16, 1513 (1979).
[5]J. N. Schulman and T. C. McGill, Phys. Rev. B 19, 6341 (1979).
[6]A. Madhukar, N. V. Dandekar, and R. N. Nucho, J. Vac. Sci. Technol. 16, 1507 (1979).
[7]W. E. Pickett and M. L. Cohen, J. Vac. Sci. Technol. 15, 1437 (1978).
[8]G. C. Osbourn and D. L. Smith, Phys. Rev. B 19, 2124 (1979).
[9]E. I. Blount, Solid State Phys. 13, 305 (1962).
[10]V. Heine, Proc. Phys. Soc. 81, 300 (1963).
[11]S. L. Kurtin, T. C. McGill, and C. A. Mead, Phys. Rev. B 3, 3368 (1971).
[12]R. Dingle, W. Wiegmann, and C. H. Henry, Phys. Rev. Lett. 33, 827 (1974).
[13]R. Dornhaus and G. Nimtz, *Springer Tracts in Modern Physics* (Springer, New York, 1976), Vol. 78.
[14]E. O. Kane, J. Phys. Chem. Solids 1, 249 (1957).